



Universiteit  
Leiden  
The Netherlands

## Inherited retinal degenerations: clinical characterization on the road to therapy

Talib, M.

### Citation

Talib, M. (2022, January 25). *Inherited retinal degenerations: clinical characterization on the road to therapy*. Retrieved from <https://hdl.handle.net/1887/3250802>

Version: Publisher's Version

License: [Licence agreement concerning inclusion of doctoral thesis in the Institutional Repository of the University of Leiden](#)

Downloaded from: <https://hdl.handle.net/1887/3250802>

**Note:** To cite this publication please use the final published version (if applicable).

# 2.2

## **CRB1-associated retinal dystrophies in a Belgian cohort: genetic characteristics and long-term clinical follow-up**

Mays Talib, MD<sup>1</sup>, Caroline Van Cauwenbergh, PhD<sup>2,3</sup>, Julie De Zaeytijd, MD<sup>2</sup>, David Van Wynsberghe, MD<sup>4</sup>, Elfride De Baere, MD, PhD<sup>3</sup>, Camiel JF Boon, MD, PhD<sup>1,5</sup>, Bart P Leroy, MD, PhD<sup>2,3,6,7</sup>

*Br J Ophthalmol* 2021; online ahead of print

---

1 Department of Ophthalmology, Leiden University Medical Centre, Leiden, The Netherlands.

2 Department of Ophthalmology, Ghent University and Ghent University Hospital, Ghent, Belgium.

3 Center for Medical Genetics, Ghent University and Ghent University Hospital, Ghent, Belgium.

4 Department of Ophthalmology, Maria Middelaers General Hospital, Ghent, Belgium.

5 Department of Ophthalmology, Amsterdam UMC, Academic Medical Center, University of Amsterdam, Amsterdam, The Netherlands.

6 Division of Ophthalmology, The Children's Hospital of Philadelphia, Philadelphia, PA, USA.

7 Centre for Cellular & Molecular Therapeutics, The Children's Hospital of Philadelphia, Philadelphia, PA, USA.

## ABSTRACT

**Aim:** To investigate the natural history in a Belgian cohort of *CRB1*-associated retinal dystrophies.

**Methods:** An in-depth retrospective study focusing on visual function and retinal structure.

**Results:** Forty patients from 35 families were included (ages: 2.5-80.1 years). In patients with a follow-up of >1 year (63%), the mean follow-up time was 12.0 years (range: 2.3-29.2). Based on patient history, symptoms and/or electroretinography, 22 patients (55%) were diagnosed with retinitis pigmentosa (RP), 15 (38%) with Leber congenital amaurosis (LCA) and 3 (8%) with macular dystrophy (MD), the latter being associated with the p.(Ile167\_Gly169del) mutation (in compound heterozygosity). MD later developed into a rod-cone dystrophy in one patient. Blindness at initial presentation was seen in the first decade of life in LCA, and in the fifth decade of life in RP. Eventually, 28 patients (70%) reached visual acuity-based blindness (<0.05). Visual field-based blindness (<10°) was documented in 17/25 patients (68%). Five patients (13%) developed Coats-like exudative vasculopathy. Intermediate/posterior uveitis was found in three patients (8%). Cystoid maculopathy was common in RP (9/21; 43%) and MD (3/3; 100%). Macular involvement, varying from retinal pigment epithelium alterations to complete outer retinal atrophy, was observed in all patients.

**Conclusion:** Bi-allelic *CRB1* mutations result in a range of progressive retinal disorders, most of which are generalised, with characteristically early macular involvement. Visual function and retinal structure analysis indicates a window for potential intervention with gene therapy before the fourth decade of life in RP and the first decade in LCA.

## INTRODUCTION

Inherited retinal dystrophies (IRDs) comprise a genetically and clinically heterogeneous group of disorders, characterised by progressive degeneration of photoreceptors. The most severe form of IRD is Leber congenital amaurosis (LCA), with an estimated prevalence of 1:33.000 - 1:81.000.<sup>1</sup> <sup>2</sup> LCA presents in infancy with nystagmus and aberrant or absent visual behaviour, and poor pupillary responses. The electrophysiological responses are non-detectable from birth. The most common form of IRD, however, is retinitis pigmentosa (RP), occurring in approximately 1:3.000 - 1:4.000 worldwide.<sup>3</sup> RP is characterised by a progressive rod-cone degeneration, leading to isolated night blindness initially, followed by progressive (mid)peripheral visual field loss, and eventually some degree of central visual loss.

Mutations in the *CRB1* gene account for 7%-17% of LCA cases, and 3%-9% of isolated, non-syndromic, autosomal recessive RP patients, depending on geographic location, making it one of the most common genetic causes of both LCA and RP.<sup>4, 5</sup> *CRB1* mutations are further associated with rare cases of cone-rod dystrophy or macular dystrophy (MD).<sup>6, 7</sup> To date, more than 230 pathogenic variants in *CRB1* have been reported,<sup>8</sup> and some genotype-phenotype correlations have emerged.<sup>9, 10</sup> Relatively few clinical cohorts have been described thus far.<sup>9, 11</sup> In the largest clinical long-term follow-up cohort published thus far, we have described 55 patients, who were found to have either *CRB1*-associated RP or LCA, and we found the window of therapeutic opportunity to be in the first three decades of life in RP, while LCA presented with much earlier blindness.<sup>9</sup>

Although for most IRDs no effective and approved treatment is currently available, the recent approval of subretinal gene therapy for *RPE65*-associated IRDs presents a promising perspective for other candidate genes.<sup>12</sup> One such candidate gene is *CRB1*, for which retinal gene therapy has shown efficacy in rescuing the retinal structure and function in mouse models.<sup>13</sup> As human subretinal gene therapy is being developed for *CRB1*-associated retinopathies, a full understanding of the natural disease course, clinical variability and potential genotype-phenotype correlations in diverse patient populations is essential to provide patients and their families with an accurate prognosis, to assess the best clinical endpoints for future trials, and to enable consequent efficient patient selection for treatment. The aim of the present study was to investigate the natural history and longitudinal characteristics in a large cohort of Belgian patients with *CRB1*-associated IRDs.

## METHODS

### Subjects and data collection

This study identified patients with *CRB1*-associated IRDs, who underwent  $\geq 1$  clinical examination. Inclusion criteria were molecular confirmation of two likely disease-causing variants in *CRB1*,

or a clinical diagnosis of IRD in a patient with a sibling with two molecularly confirmed likely disease-causing variants in *CRB1*. This study was approved by the ethics committee of the Ghent University Hospital, and adhered to the tenets of the Declaration of Helsinki. The local ethics committee waived the need for informed consent on the condition of pseudonymisation.

All patients were seen in the ophthalmic genetics outpatient clinics at the department of ophthalmology of Ghent University Hospital in Belgium, the national referral centre for genetic eye diseases. A standardised retrospective analysis of existing medical records was performed for data collection of the ophthalmic history, including the age at symptom onset and/or age at diagnosis, best-corrected visual acuity (BCVA), slit-lamp biomicroscopy, funduscopy with white light fundus pictures, manual Goldmann visual fields (GVF), colour vision testing, full-field dark-adapted and light-adapted single flash and 30 Hz ISCEV standard electroretinography (ERG),<sup>14</sup> spectral-domain optical coherence tomography (SD-OCT) and fundus autofluorescence (FAF) where available. SD-OCT and FAF images were obtained with the Heidelberg Spectralis (Heidelberg Engineering, Heidelberg, Germany). GVF areas of the V4e and I4e targets were digitised and converted to seeing retinal areas in mm<sup>2</sup>, using a method described by Dagnelie.<sup>15</sup>

Diagnostic criteria for LCA were (1) aberrant or absent visual behaviour or severe visual impairment from infancy, with or without nystagmus, and (2) non-detectable dark-adapted and light-adapted amplitudes on ERG in the first year of life, if available.

### **Molecular diagnosis**

Of the 40 subjects, 38 (95%) had received a molecular diagnosis through different approaches over the course of 10 years (2007-2017), which comprised arrayed primer extension microarray chip (APEX chip, Asper Bio, Tartu, Estonia) including; LCA chip (n = 5), autosomal recessive (ARRP) chip (n = 4), gene and LCA panel analysis using Sanger sequencing (n = 8 and n = 4, respectively), next-generation sequencing (n = 8, ERD4000, n = 3), a combination of Sanger sequencing with LCA chip (n = 4) or ARRP chip (n = 1), or a combination of LCA chip and LCA panel (n = 1). Mutational analyses were either performed at the Ghent University Hospital in Belgium, or at the Manchester Centre for Genomic Medicine. There were no subjects with mono-allelic *CRB1* mutations included in this study. Carrier status testing with Sanger sequencing confirmed mono-allelic *CRB1* variants in all available family members (n = 24) of confirmed patients. Clinical data was available for 3 out of 24 carrier family members, showing no ophthalmological abnormalities.

### **Statistical analysis**

Data were analysed using SPSS V.23.0. For normally distributed data, means and SD were used. For non-normally distributed data, medians and IQR were used. Longitudinal analysis of Snellen BCVA and the seeing retinal area were performed using linear mixed models, using the logarithmic transformation of these parameters, that is, the logarithm of the minimum angle of resolution

(logMAR) and the logarithmic conversion of the seeing retinal area. Visual endpoints were low vision (BCVA  $<0.3$  and  $\geq 0.1$ , and/or visual field diameter  $<20^\circ$ ), severe visual impairment (BCVA  $<0.1$  and  $\geq 0.05$ ) and blindness (BCVA  $<0.05$ , and/or visual field diameter  $<10^\circ$ ), based on WHO criteria. In our analysis of visual fields, we added a category of mild visual field-based impairment ( $20^\circ \leq$  visual field diameter  $<70^\circ$ ). Intra-individual asymmetry in BCVA was defined as a between-eye difference of  $\geq 15$  Early Treatment Diabetic Retinopathy Study letters (logMAR scale). In cases where the patient was blind in both eyes, the last examinations prior to reaching blindness were used, in order to avoid a floor effect.

## RESULTS

Of the 40 patients who were included from 35 families (online supplemental figure 1), 25 (63%) had follow-up of longer than 1 year (median follow-up time: 12.0 years; IQR: 16.3; range: 2.3-29.2 years). Six patients (15%) were from consanguineous families, and only 2 of these (ID-2 and ID-13) were compound heterozygous. Based on initial symptomatology and ERG results, 22 patients (55%) had RP and 15 patients (38%) had LCA. Three patients (8%) had an isolated MD, one of whom (ID-36) was initially misdiagnosed as a central areolar choroidal dystrophy. The mean age at last examination was 35.2 years (SD: 20.3; range: 2.5-80.1 years). The clinical characteristics are listed in table 1.

Thirty distinct mutations were found (online supplemental table 1), with most mutations clustering in exon 6 (20% of mutations) and exon 7 (23% of mutations). Three patients carried the c.498\_506del p.(Ile167\_Gly169del) mutation in compound heterozygous form, and they had isolated MD, which progressed to mild rod-cone dystrophy, based on full-field ERG findings in patient ID-33, while the peripheral retina maintained a normal appearance on funduscopy. In the group of patients who had a truncating mutation on  $\geq 1$  allele, LCA was not significantly more prevalent than RP ( $p = 0.10$ ).

### Disease onset and visual function

Data on the age at symptom onset or at diagnosis were available for 31/40 patients (78%). The median age at symptom onset or diagnosis was during the first year of life for patients with LCA (IQR: 0.75; range: first year of life-3 years), 5 years for patients with RP (IQR 6.0; range: first year of life-26 years), and 18 years for patients with (initial) isolated MD (range 7-23 years). Of note, the early age at symptom onset seen in patients with RP is based on symptoms of nyctalopia, whereas the age at onset in patients with LCA is based on non-detectable ERG responses, nystagmus and/or reports of severe vision loss in the first years of life. In RP, 3/15 patients (20%) presented with symptoms or received their diagnosis after the first decade of life. Two patients with RP, ID-9 and ID-14, presented initially with an intermediate or panuveitis, at the ages of 26 and 5 years,

respectively. They were treated with intravitreal injections of anti-vascular endothelial growth factor and adalimumab (ID-9), which led to either no or only very limited improvement, and intravitreal triamcinolone injections (ID-14), which elicited secondary glaucoma.

**Table 1. Clinical characteristics of patients with *CRB1*-associated IRDs**

Characteristics*	RP (n = 22)	LCA (n = 15)	MD (n = 3)
Age at last examination (years; mean $\pm$ SD)	33.8 $\pm$ 21.5	38.7 $\pm$ 22.0	32.1 $\pm$ 4.9
Age at symptom onset or diagnosis (years; mean $\pm$ SD)	7.2 $\pm$ 6.4	0.2 $\pm$ 0.4	16.0 $\pm$ 8.2
Follow-up time (years; median (IQR))	2.8 (14.6)	2.8 (7.9)	13.9 (-)
Western European ethnicity†	19 (86)	12 (80)	3 (100)
<b>Spherical equivalent refractive error available, n</b>	<b>12</b>	<b>7</b>	<b>3</b>
Mean $\pm$ SD, D	+2.5 $\pm$ 1.9	+6.5 $\pm$ 1.5	+0.5 $\pm$ 1.9
Range	-0.3 to +5.9	+4 to +9	-1.1 to +2.6
-1 D to 0 D, n (%)	1 (8)	-	2
0-2 D, n (%)	4 (33)	-	-
2-4 D, n (%)	4 (33)	-	1
4-6 D, n (%)	3 (25)	2 (29)	-
$\geq 6$ D, n (%)	-	5 (71)	-
Nystagmus present, n (%)	6 (27)	13 (87)	0 (0)
Shallow anterior chamber, n (%)	5/9 (56)	1/3 (33)	0/2
Cataract, n (%)	11 (52)	3 (20)	-
Keratoconus with stromal cicatrization, n (%)	-	2 (13)	-
Enophthalmos‡, n (%)	-	6 (40)	-
<b>Vitreous abnormalities, n (%)</b>	<b>4 (19)</b>	<b>1 (13)</b>	<b>1 (33)</b>
Cells	1	-	1
Synchysis scintillans	3	1	-
<b>Fundoscopy examination, n (%)</b>			
Optic disc pallor	13 (62)	5 (33)	2 (67)
Optic disc hyperaemia	2 (9)	1 (13)	-
Pseudopapillary oedema	1 (5)	2 (25)	-
Macular RPE alterations/atrophy §	20/20 (100)	12/12 (100)	3 (100)
Spicular intraretinal pigmentation	10 (48)	1 (13)	-
Nummular intraretinal pigmentation	8 (36)	9 (60)	-
Vascular attenuation	12 (55)	4 (27)	1 (13)
PPRPE	8 (36)	7 (47)	1 (33)
Fine yellow drusenoid deposits	10 (45)	7 (47)	2 (67)

\*Clinical characteristics at the last examination were used.

†In the LCA group, 2 patients were Eastern-European; 1 was Southern-European. In the RP group, 1 patient was Middle-Eastern, 1 patient was Black, and 1 was Southeast Asian.

‡This was due to atrophy of peri-orbital tissue, associated with frequent eye rubbing/poking.

§ Alteration or atrophy of the macular retinal pigment epithelium (RPE) was observed in 35 patients (88%). In the remaining 5 patients, who were blind (BCVA range no light perception – light perception), the macula could not be evaluated due to dense cataract (n = 2), synchysis scintillans (n = 1), miosis due to posterior synechiae, or phthisis bulbi (n = 1).

BCVA, best-corrected visual acuity; D, dioptres; LCA, Leber congenital amaurosis; MD, macular dystrophy; PPRPE, preservation of the para-arteriolar retinal pigment epithelium; IRDs, inherited retinal dystrophies; RPE, retinal pigment epithelium.

Figure 1 shows the proportion of patients in each category of visual impairment at the initial visit, based on BCVA and visual fields, against age. During follow-up, 28 patients (70%) reached BCVA-based blindness, 14 of whom had LCA, 13 of whom had RP and 1 had MD. Visual field-based blindness was documented in 17/25 patients (68%). Of these patients, 15 (38%) were blind based on both BCVA and visual field. Intra-individual asymmetry in BCVA was found in 13 patients (33%). The presumed cause of asymmetry was determined in 10 patients (online supplemental table 2).

The rate of BCVA decline in the better-seeing eye was 15.2%/year in patients with RP ( $p < 0.0000001$ ) and 8.2%/year in patients with LCA ( $p = 0.002$ ). In the worse-seeing eye, these rates were 16.9% ( $p < 0.0000001$ ) and 5.7% ( $p = 0.013$ ), respectively.

GVFs were available for 25 patients (55%), 14 of whom had follow-up GVFs with a mean follow-up time of 11.5 years (SD: 6.4; range: 4.0–24.4). The rates of visual field decline for the V4e and I4e isopter in the better-seeing eye was 16.0%/year ( $p < 0.0001$ ) and 20.1%/year ( $p = 0.002$ ) in patients with RP, respectively. In the worse-seeing eye, these rates were 20.4%/year ( $p < 0.0001$ ) and 21.3%/year ( $p = 0.0004$ ) in patients with RP. In patients with LCA, the visual field decline for the V4e isopter was 18.9%/year, while the other parameters were too affected at baseline to allow reliable calculation of the decline rate. The number of patients with MD was too low to calculate reliable decline rates for BCVA or visual fields.

### Ophthalmic and fundus findings

The mean spherical equivalent of the refractive error at the last examination was +3.7 D (SD: 2.8; range: -1.1 D to +9.0 D), and hyperopia was present in 16/22 patients (73%) with available data on the refractive error. The only patient with myopia (spherical equivalent  $< -0.75$  D) had an isolated MD phenotype. Angle-closure glaucoma was diagnosed in three patients (8%; one with LCA and two with RP), and was treated with a surgical peripheral iridectomy in two cases, one of whom also received cataract surgery and with laser peripheral iridotomy in one case. One additional patient received prophylactic peripheral iridotomy due to a shallow anterior chamber, and one patient had received a surgical peripheral iridectomy, the indication for which could not be retrieved from the available clinical history. Patient ID-32 was diagnosed with uveitis and angle closure due to



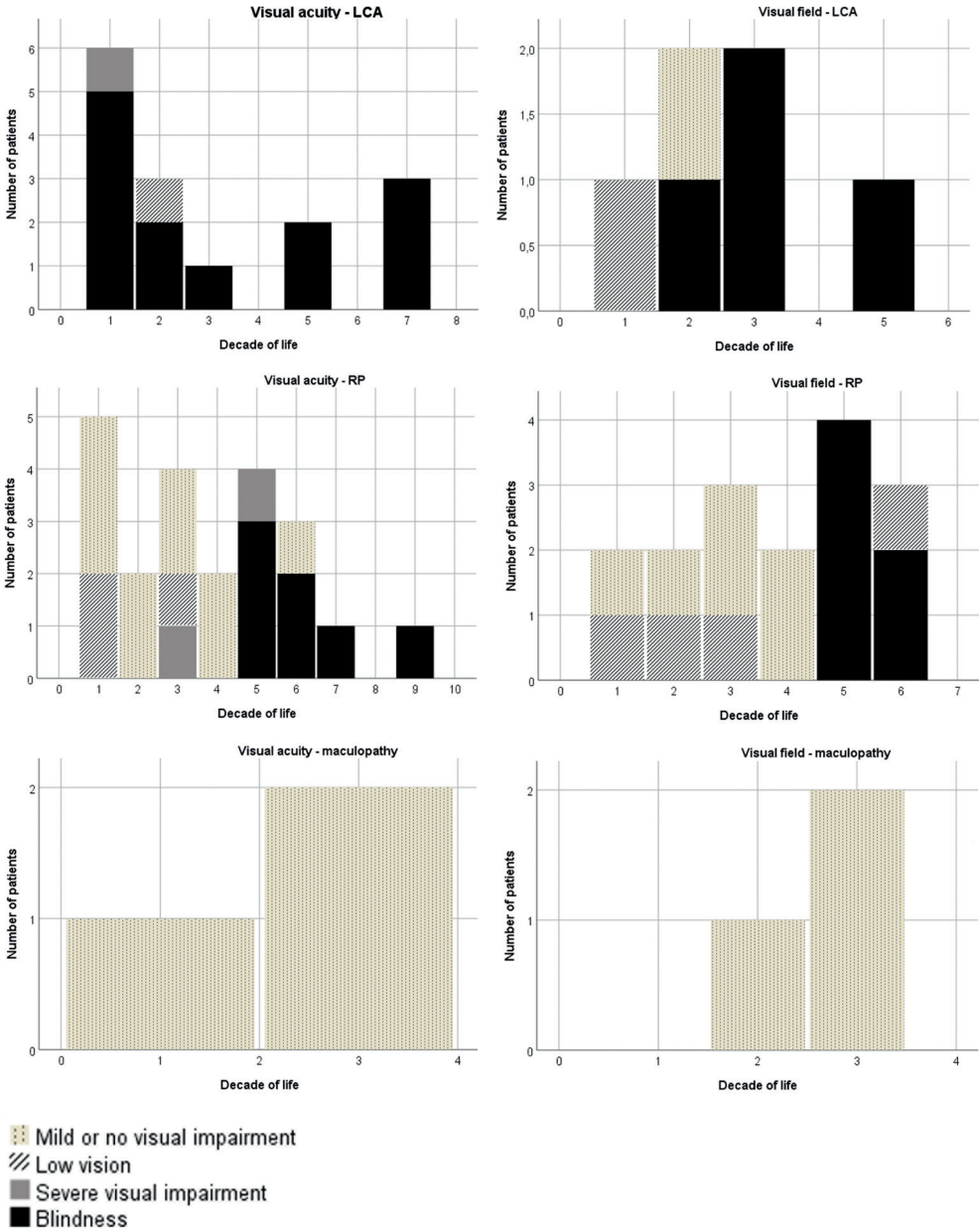


**Figure 1. Visual function in CRBI-associated retinal degenerations, stratified by diagnosis.** Data were collected from the initial visit, and the better-seeing eye was used for this analysis. Panels on the left indicate visual impairment based on best-corrected visual acuity (BCVA), showing mild or no visual impairment (BCVA  $\geq 0.3$ ), low vision (BCVA  $< 0.3$ ), severe visual impairment (BCVA  $< 0.1$ ), and blindness (BCVA  $< 0.05$ ), based on WHO criteria. Panels on the right indicate visual impairment based on visual field, showing no visual impairment (visual field diameter  $\geq 70^\circ$ ), mild visual impairment (diameter  $< 70^\circ$ ), low vision (diameter  $< 20^\circ$ ), or blindness (diameter  $< 10^\circ$ ). The graphs

show visual impairment with advancing age in patients with *CRB1*-associated Leber congenital amaurosis (LCA) in the top row, for *CRB1*-associated retinitis pigmentosa (RP) in the second row, and for *CRB1*-associated macular dystrophy (MD) in the third row. In LCA, BCVA-based blindness is common from the first decade of life, but some visual field may still be intact. In RP, BCVA-based as well as visual field-based blindness is common from the fifth decade of life onward. In MD, BCVA and visual field are well-preserved, although the few patients in this population were still young at the final visit.

seclusio pupillae at the age of 54 years, and was treated with diode laser cyclodestruction, followed by trabeculectomy. Optic disc drusen (5/40 patients; 13%) or hamartomas (1/40 patients; 3%) were found in patients with LCA ( $n = 1$ ) and RP ( $n = 5$ ), who had mutations in *CRB1* exons 5-9. Alterations or atrophy of the macular retinal pigment epithelium (RPE) were universal (table 1).

Intraretinal pigment migrations were present in 36/40 patients (90%). Nummular pigmentations were much more frequent than those of the spicular type in LCA patients (7/8 patients). Nummular pigmentations were present in 7/21 RP patients (33%). Of the patients without intraretinal pigment migrations, 3 had an isolated MD phenotype, and one patient had RP but was aged 6 years at the last examination. The earliest fundus changes were found in patient ID-13 (RP), at the age of 11 months, and consisted of mild macular RPE alterations only. Macular pseudocoloboma was observed in three patients with LCA. Preservation of the peri-arteriolar retina and RPE was present in 16/40 patients (40%), across all diagnostic groups (table 1). Fine yellow punctate deposits in the peripheral retina were present in 19/40 patients (48%). Patients ID-1 and ID-31 had a unilateral and bilateral retinal detachment, respectively. The underlying cause was Coats-like vasculopathy in ID-1, and not documented in ID-31.

### Full-field ERG

Full-field ERGs, available for 16 patients (40%), were non-detectable in 3/3 patients with LCA. One patient with LCA (ID-24) had some remaining light-adapted responses in his first year of life, despite having only light perception vision. Dark-adapted and light-adapted responses were extinguished in 5/9 patients with RP at the first ERG examination (ages: 4-40 years), while others had a rod-cone pattern of dysfunction. Three patients with MD had normal dark-adapted and light-adapted ERG responses. One of these patients, patient ID-33, who had no generalised panretinal dysfunction on ERG between the ages of 23 years and 26 years, had developed a mild rod-cone dystrophy by the age of 28 years.

**Table 2. Integrity of photoreceptor layers on SD-OCT in patients with *CRB1*-associated IRDs**

<b>Retinitis pigmentosa</b>		<b>N</b>	<b>Age (years)</b>
EZ	Granular or attenuated in peripheral macula, with relative sparing in fovea	4/12*	14-54
	(Nearly) unidentifiable in peripheral macula, but sparing in the fovea	3/12	35-43
	(Nearly) unidentifiable in entire macula	5/12	5-80
ELM	(Nearly) unidentifiable or severely attenuated in peripheral macula, with foveal sparing	6/12	14-54
	(Nearly) unidentifiable in entire macula	6/12	5-80
ONL	Normal thickness or only mild attenuation in entire macula	1/12	54
	Normal thickness or mild attenuation in fovea, with more severe attenuation in peripheral macula	2/12	14-16
	Severe attenuation in entire macula	3/12	5-40
	(Nearly) unidentifiable in entire macula	5/12	35-80
	Severe attenuation in fovea, with sparing in peripheral macula	1/12	26
<b>Leber congenital amaurosis</b>		<b>N</b>	<b>Age (years)</b>
EZ	Fully unidentifiable in entire macula	1/6	11
	Unidentifiable in peripheral macula, nearly unidentifiable in fovea	2/6	4-7
	Unidentifiable in fovea, nearly unidentifiable in peripheral macula	3/6	3-20
ELM	Fully unidentifiable in entire macula	5/6	3-20
	Some foveal sparing (nearly unidentifiable)	1/6	7
ONL	Severely attenuated or (nearly) unidentifiable in entire macula	6/6	3-20
<b>Macular dystrophy</b>		<b>N</b>	<b>Age (years)</b>
EZ	Somewhat granulated in peripheral macula, with sparing in the fovea	1/3	26
	Sparing in the peripheral macula and fovea, with atrophy in the parafovea (bull's eye maculopathy) †	1/3	29
	Almost absent in fovea, sparing in peripheral macula	1/3	31
ELM	Good quality in fovea and peripheral macula	1/3	26
	Good quality in fovea, granulated in peripheral macula†	1/3	29
	Unidentifiable in fovea, good preservation in peripheral macula	1/3	31
ONL	Normal in entire macula	1/3	26
	Severe attenuation with some foveal sparing†	1/3	29
	Severe attenuation, more atrophy in fovea	1/3	31

\*Six patients (one with LCA; five with RP) who had undergone SD-OCT imaging were not included in this table, as either only single scans or only descriptions of the images were available in the medical records, describing atrophy of the outer retina and photoreceptor layers.

†This was patient ID-33, who later developed rod-cone dystrophy. The pattern of atrophy on SD-OCT did not change, although the atrophy was progressive.

ELM, external limiting membrane; EZ, ellipsoid zone; IRDs, inherited retinal dystrophies; LCA, Leber congenital amaurosis; MD, macular dystrophy; ONL, outer nuclear layer; RP, retinitis pigmentosa; SD-OCT, spectral-domain optical coherence tomography.

**Retinal imaging**

SD-OCT data (see table 2), available for 27 patients (68%), showed inner retinal thickening (21/27; 78%), cystoid macular oedema (CMO; 14/27; 52%; unilateral in 3 cases), and disorganization of the lamellar retinal structure (14/27; 52%). The other patients maintained an intact lamellar retinal structure, where despite a mildly coarse aspect (8/27; 30%), each individual retinal layer was discernible throughout the macula. Online supplemental table 3 shows the treatment regimens for CMO, which in two cases disappeared spontaneously. Conversely, patient ID-13 had no CMO until the age of 11 years, and developed bilateral CMO at the age of 12 years. An epiretinal membrane was present in 13 patients (48%), and was mild in 9 patients, but formed a pucker in 4 patients. A unilateral lamellar hole was present in patient ID-9, which later developed into a full-thickness macular hole.

Blue-light (short wavelength) autofluorescence imaging (SWAF) was performed in 20 patients (50%). Six of those had either nystagmus ( $n = 5$ ) and/or were blind in both eyes ( $n = 5$ ), so that it was impossible to obtain interpretable SWAF images. In the others, SWAF showed variable patterns (Figures 2 and 3), with relative sparing of the foveal autofluorescence in eight patients.

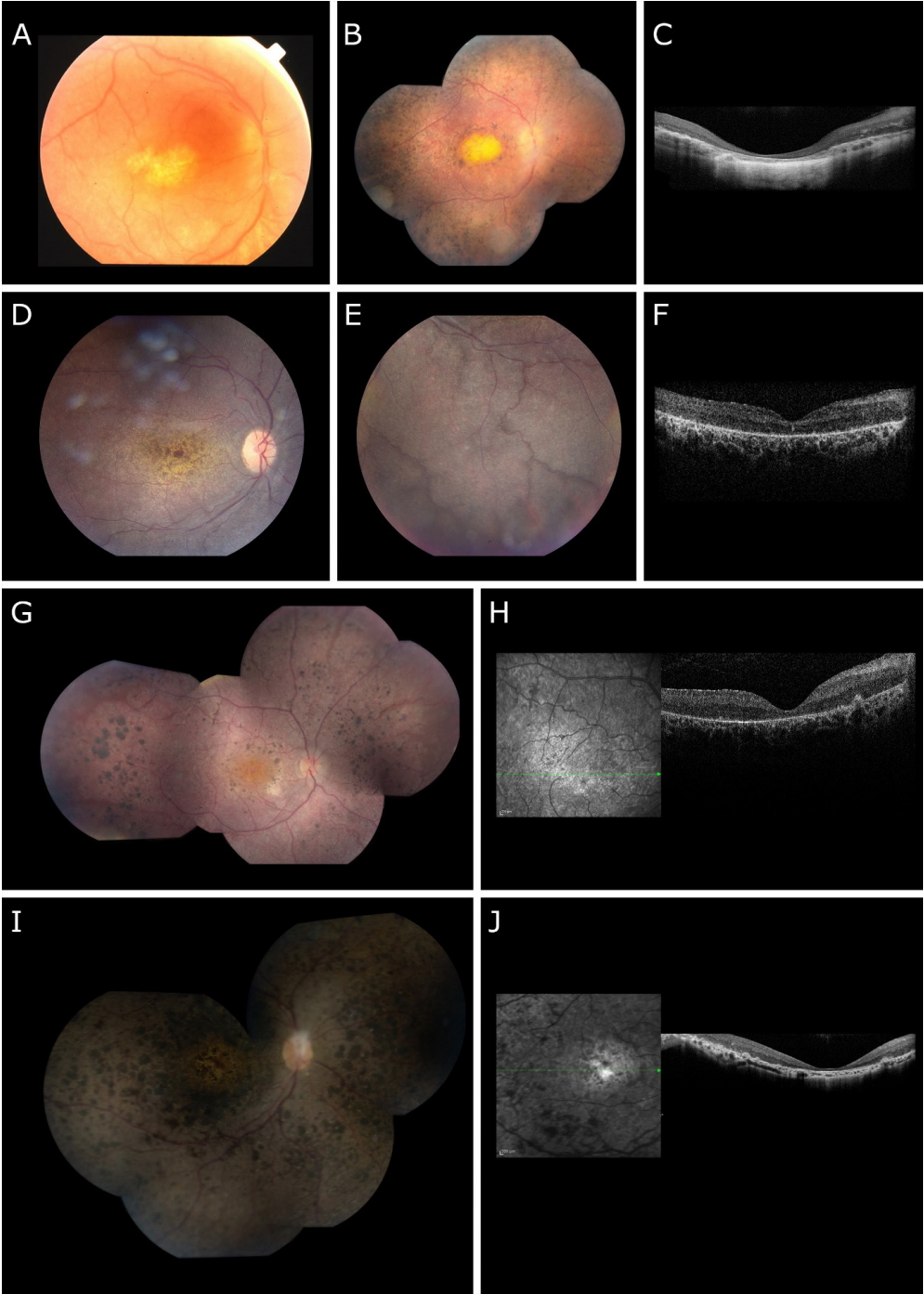


Figure 2. Imaging in *CRB1*-associated Leber congenital amaurosis (LCA) or retinitis pigmentosa (RP). A-C. Long-term disease progression in a patient with LCA. At the age of 6 years (A), an area of outer retinal atrophy

including the retinal pigment epithelium (RPE) was observed in the central macula (decimal best-corrected visual acuity (BCVA) of the right eye (OD): 0.03). The periphery (not shown here) had a salt-and-pepper aspect, but no obvious spicular hyperpigmentation. At the age of 25 years (B), the central atrophic area had grown into what was described as a macular pseudocoloboma (BCVA OD: hand motion vision), and mixed intraretinal nummular and spicular pigmentation migration extended from the periphery into the posterior pole. White-yellow drusenoid deposits are visible in the midperiphery, similar to the deposits seen in *CRB1*-associated retinitis pigmentosa (Figure 3). Spectral-domain optical coherence tomography (SD-OCT) (C) showed profound atrophy of outer retinal layers. The external limiting membrane (ELM) and ellipsoid zone (EZ) were undetectable. On short-wavelength fundus autofluorescence imaging (not shown here), no autofluorescence signal could be detected. Decimal BCVA was 0.03.

**D-F.** A 7-year-old patient with RP, whose sibling had LCA. The fundus (D) showed a yellow profound macular atrophy, with some foveal preservation (BCVA OD: 0.4; left eye (OS): 0.06). Note the white-yellow drusenoid deposits in the macula, also abundant in the (mid)periphery. The periphery (E) showed pronounced para-arteriolar preservation of the RPE (PPRPE), a feature typical of *CRB1*-associated retinopathies. Nummular intraretinal hyperpigmentation (not shown here) was present, but sparse. SD-OCT (F) showed atrophy of the outer retinal layers. No identifiable ELM or EZ could be discerned, and only small hyperreflective tufts were scattered along the macula.

**G-H.** An 11-year-old patient with LCA. Composite fundus photography (G) shows yellowish atrophy of the macula, nummular intraretinal pigmentation in the perimacular region and the periphery (BCVA OD: 0.03), and PPRPE in the periphery. In the papillomacular region, fibrous scar tissue formation is visible. This fibrous tissue was present to a greater extent in the other eye, in the same papillomacular region. The SD-OCT (H) shows inner retinal thickening, and severe outer retinal atrophy, with some remaining outer nuclear layer, but no identifiable ELM or EZ.

**I-J.** A 12-year-old patient with LCA. The fundus (I) shows optic disc drusen (note irregular optic disc border), profound retinal atrophy (BCVA OU: finger counting vision) and panretinal nummular hyperpigmentation. Yellow drusenoid deposits are visible throughout the retina. A coincidental finding is the Bergmeister optic disc, seen as the small tuft of fibrous tissue on the optic disc. The SD-OCT (J) shows no evident inner retinal thickening, but profound atrophy of the outer retina, particularly in the fovea. No identifiable ELM or EZ is visible.



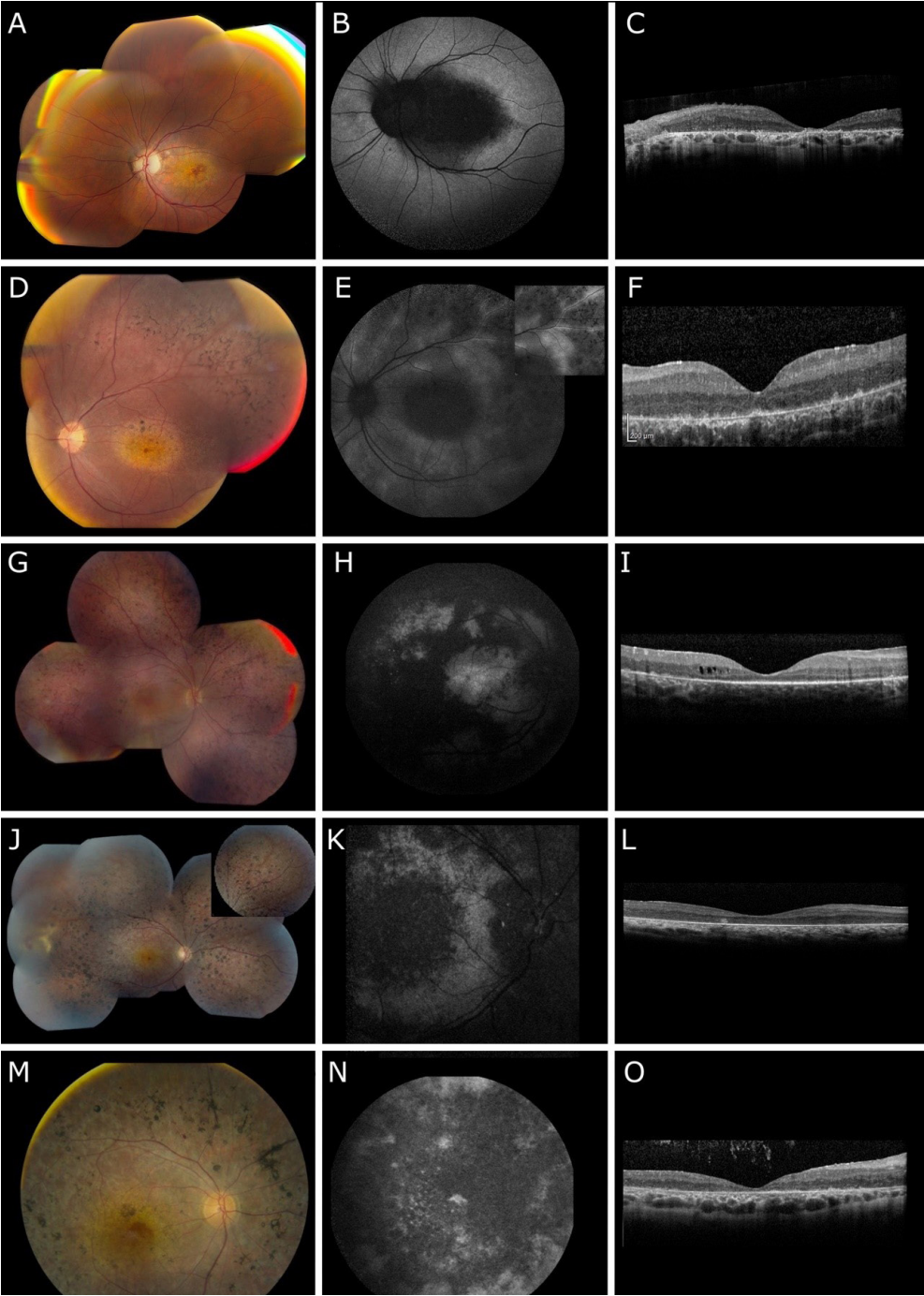


**Figure 3.** Multimodal imaging in patients with *CRB1*-associated macular dystrophy (MD) or retinitis pigmentosa (RP). A-C. A 36-year-old patient with an isolated MD, which was initially diagnosed as central areolar

choroidal dystrophy. Composition fundus photography (A) shows chorioretinal atrophy in the central macula, with relative sparing of the fovea. The peripheral macula and the retinal (mid)periphery, including the vasculature, appear entirely normal. The short-wavelength fundus autofluorescence (FAF) image (B) shows severely reduced to absent autofluorescence in the corresponding area of the macula. Spectral-domain optical coherence tomography (SD-OCT) scan (C) shows profound atrophy of the outer nuclear layer (ONL) and the hyperreflective outer retinal bands (external limiting membrane and ellipsoid zone), and a near absence thereof in the fovea. The decimal best-corrected visual acuity (BCVA) was 0.01 in this eye. **D-F.** A 14-year-old patient with RP. The fundus (D) shows a distinctive, yellow, relatively circumscribed area of macular atrophy, with small areas of foveal and parafoveal sparing, which explains a BCVA of 0.5 in this eye. In the superotemporal periphery, para-arteriolar preservation of the retinal pigment epithelium (PPRPE) is seen, a feature highly typical of *CRB1*-associated RP. Spicular intraretinal pigmentation is seen in the periphery, along with small, yellowish, drusenoid deposits. FAF (E) shows severe hypo-autofluorescence in the macula, and strokes of reduced FAF in the midperiphery. Autofluorescence is relatively preserved in the peripheral macula and around the arterioles (picture-in-picture). SD-OCT (F) shows inner retinal thickening, outer retinal atrophy, and relative preservation of the ONL and the hyperreflective outer retinal bands in the fovea. **G-I.** A 16-year-old patient with RP. The fundus (G) shows extensive bone-spicule hyperpigmentation in the periphery, extending into the temporal posterior pole, with a spared central macula. FAF (H) confirms this pattern, showing normal autofluorescence in the central macula and severely reduced FAF in the remaining posterior pole and midperiphery. Patches of relative preservation are scattered in the superior midperiphery. SD-OCT (I) shows relative foveal preservation of the ONL and the hyperreflective outer retinal bands. The ellipsoid zone seemed more preserved than the external limiting membrane. Mild cystoid macular oedema was visible in the temporal parafovea. BCVA was 0.5. **J-L.** A 26-year-old patient with RP and Coats-like exudative vasculopathy. The fundus (J) shows a pale optic disc, and the distinct yellow coloration of the atrophic macula, with relative foveal sparing. A greyish reticular pattern of outer retinal atrophy is seen in the posterior pole and the nasal (mid)periphery. Nummular intraretinal pigmentation is seen. PPRPE is particularly visible in the nasal and superior quadrants. White drusenoid deposits are scattered in atrophic as well as in relatively preserved areas (picture-in-picture). The Coats-like exudate is seen in the temporal periphery. FAF (K) shows profound hypo-autofluorescence in the central macula and midperiphery, with relative sparing in the peripheral posterior pole. The SD-OCT scan (L) shows atrophy of the ONL and the hyperreflective outer retinal bands. The BCVA in this eye was 0.05. **M-O.** A 45-year-old patient with RP. The fundus (M) shows yellowish areas of macular atrophy with foveal sparing. Extensive nummular pigmentation, along with a greyish reticular pattern of outer retinal atrophy, is seen in the midperiphery, extending into the posterior pole. FAF (N) shows generalised mottled hypo-autofluorescence with limited patchy regions of preserved autofluorescence. FAF in the fovea is attenuated. SD-OCT (O) shows atrophy of the ONL and the hyperreflective outer retinal bands, which are not evidently identifiable. The inner retina is mildly thickened. The BCVA in this eye was 0.2.

## DISCUSSION

In this retrospective cohort study, we detail the natural disease course and clinical spectrum of *CRB1*-associated IRDs in a large Belgian cohort of 40 patients from 35 families. Patients were evaluated extensively with functional testing and multimodal imaging, with a follow-up time up to 29 years. We elucidate several genotype-phenotype correlations.

In this study, 55% of patients had an RP diagnosis, 8% had an MD, while the other patients presented with the more severe LCA (38%). In previous literature, the terms LCA and early-onset severe



retinal dystrophy (EOSRD) have been used interchangeably to some extent.<sup>16</sup> The phenotypes were more severe in this Belgian cohort than in the previously published Dutch cohort, where LCA comprised only 9% of the *CRB1*-RD population.<sup>9</sup> Within the RP groups, however, findings were relatively similar. The median age at symptom onset for patients with *CRB1*-RP in the current cohort was 5 years, versus 4 years in the Dutch cohort, and 20% of patients in the current cohort had a disease onset after the first decade of life, versus 15% of patients with *CRB1*-RP in the Dutch cohort.<sup>9</sup> A salient finding is the initial presentation with uveitis in two patients with RP (10%), which has been reported before in *CRB1*-associated retinopathy.<sup>17</sup> The prevalence of uveitis in any form (anterior, intermediate and posterior) in the genetically undifferentiated RP population has been estimated at 0.26%,<sup>18</sup> although some studies have shown a higher prevalence of inflammatory activity in patients with RP in the vitreous cavity (37%), indicating an association between RP and inflammation.<sup>19</sup>

Besides typical RP-associated fundus hallmarks, distinctive features included fine yellow punctate spots, found in 48%, and which have been noted in cases of patients with *CRB1*-RD,<sup>20</sup> as well as in *Crb1*<sup>rd8/rd8</sup> mutant mice, where immunostaining indicated that these spots represent subretinal microglia/microphages.<sup>21</sup> This suggests that these spots are indicative of a pro-inflammatory phenotype. Alternatively, they may represent degenerated or migrated Müller cells. The full significance and relevance of this feature remains elusive. Another distinctive characteristic was periarteriolar preservation of the RPE, which was present across all diagnoses, but was most prevalent in *CRB1*-LCA. Earlier smaller studies and case series have found early macular involvement a notable finding in *CRB1*-RP and *CRB1*-LCA.<sup>22-24</sup> In this study, macular RPE alterations or atrophy was universal in all patients where the macula could be visualised, confirming our findings in the Dutch cohort.<sup>9</sup> A particularly interesting finding is the macular pseudocoloboma in three patients with LCA. Case series have described macular (pseudo)coloboma in LCA associated mostly with mutations in *CRX* and *AIPL1*, but also with mutations in *NMNAT1*, *LCA5* (encoding Lebercilin) and *IDH3A*.<sup>25-27</sup> To the best of our knowledge, this is only the second report of macular pseudocoloboma in *CRB1*-LCA.<sup>28</sup> Coats-like exudative vasculopathy was found in 13% of patients in this cohort, similar to earlier reports.<sup>9, 29</sup> ERG responses were extinguished in 100% of LCA patients and 56% of patients with RP with available ERGs, compared to 50% of patients with RP in the Dutch cohort. This suggests that, in a future *CRB1* gene therapy trial, ERG examination may not be an appropriate outcome measure of efficacy.

The high proportion of left-censored data for low vision and blindness, that is, patients who had low vision or were blind at the initial presentation, was too high to calculate reliable survival curves in this cohort. In fact, 75% of patients in this cohort reached blindness: 70% reached BCVA-based blindness, and 68% reached visual field-based blindness, with considerable overlap. In RP, mild visual impairment was observed in the first decade of life, while both BCVA-based and visual

field-based blindness were mostly observed from the fifth decade of life and onward, corroborating observations from earlier large cohorts.<sup>9, 11</sup>

Meaningful findings on SD-OCT included inner retinal thickening (78%), and cystoid maculopathy (52%), similar to findings in the Dutch population, as well as findings in *Crb1*<sup>-/-</sup>/*Crb2*<sup>-/-</sup> mice.<sup>30</sup> Disorganization of the retinal laminar structure, however, was more prevalent: 52% in the Belgian cohort versus 9% of Dutch patients. In these patients, the amenability of the retina to subretinal gene therapy may be less likely. The results are confounded by the higher proportion of patients with *CRB1*-LCA in the Belgian population, while the few patients with *CRB1*-LCA in the Dutch population had no SD-OCTs available for analysis. In the other 48% of Belgian patients, mostly patients with RP or MD, but also two with LCA, the laminar structure of the retina was essentially maintained, despite some degree of coarseness. Other crucial biomarkers indicating amenability to gene therapy include the ellipsoid zone (EZ), external limiting membrane (ELM) and outer nuclear layer (ONL). In  $\geq 50\%$  of patients with RP, EZ and ELM were spared in the fovea (table 2). However, the ONL was more severely attenuated. This suggests that in these patients, gene therapy has some anatomical basis for potential success, as CRB1 protein supports the adhesion between photoreceptors and Müller cells at the level of the ELM.<sup>31</sup> Again, the atrophy of the photoreceptor layers on SD-OCT was more profound in the Belgian *CRB1*-RP population compared with the Dutch *CRB1*-RP population. In Belgian patients with LCA, the EZ, ELM and ONL were (nearly) unidentifiable in almost all patients. These findings were based on multiple single scans, as nystagmus or the lack of fixation challenged image capture in LCA patients, but are in keeping with the more severe nature of congenital and early-onset *CRB1*-related disease.

Non-retinal features included hyperopia (73%), a narrow anterior chamber (63% of patients with RP; 43% of total, where information on anterior chamber depth was available) and optic disc drusen or hamartomas (16%). These data propose a role for CRB1, a large and complex protein, in normal ocular development, although its precise role in this context is not known. Acute angle-closure glaucoma occurred in 8% of patients, in line with previous findings,<sup>32, 33</sup> but with a lower incidence than found in the Dutch population.<sup>9</sup>

The genotypic distribution in this cohort was decidedly different from that in the Dutch cohort. The Belgian cohort was genotypically and ethnically more diverse, as 30 distinct mutations were found, and 15% of patients were of non-Western-European descent. Meanwhile, the Dutch cohort consists largely of a genetic isolate carrying a homozygous p.(Met1041Thr) mutation, which was not present in this Belgian cohort. This genotypic difference, and particularly the higher prevalence of nonsense mutations in this cohort may hold at least part of the explanation for the contrasting phenotypic severity between this and the previously published Dutch cohort. In the current cohort, six patients had bi-allelic truncating mutations, four of whom had LCA and two had RP. In the Dutch cohort, no patient had bi-allelic truncating mutations. This partially substantiates the earlier

suggestion of an association between truncating mutations and an LCA phenotype,<sup>34</sup> although this association was not significant in this cohort ( $p = 0.10$ ).

The presence of genotype-phenotype correlations in many types of inherited IRDs, including *CRB1*-associated IRDs, has been contentious. An association between null mutations and a higher likelihood of an LCA phenotype has been suggested, due to the complete loss of *CRB1* protein.<sup>34</sup> Although we observed the trend, we could not statistically corroborate this suggestion. This study also robustly confirms the association between the p.(Ile167\_Gly169del) mutation and phenotypes predominantly affecting the macula, with or without measurable cone dysfunction on full-field ERG. A recent case series has shown this mutation in homozygous or heterozygous form in seven unrelated individuals with *CRB1*-MD.<sup>10</sup> In these patients, emmetropia or myopia is more prevalent than the typical hyperopia seen in *CRB1*-RDs.<sup>35</sup>

Although there are no therapeutic options available for patients with *CRB1*-associated RP and LCA, gene therapy is being developed, and has shown efficacy in preserving retinal structure and function in mouse models of the disease.<sup>8, 13, 36, 37</sup> Recently, an exclusive license agreement was signed between HORAMA, a French biotech company, and Leiden University Medical Centre, developer of the drug candidate (HORA-001) targeting *CRB1* mutations to treat *CRB1*-RDs.<sup>38</sup>

This study provides useful information for future (gene) therapeutic trials. Of particular interest remains the degree of intra-individual interocular symmetry, and thus comparability. This comparability is an important assumption when using the non-treated eye as a control in trials. This study found interocular asymmetry in 33% of patients, similar to the findings in the Dutch population (31%).<sup>9</sup> Yearly decline rates of BCVA and visual field area were relatively symmetric between the better- and worse-seeing eye, particularly for BCVA and the I4e isopter for the visual field. We find that the first three decades of life provide the more tenable window of opportunity for potential therapeutic intervention in patients with RP. In LCA, therapeutic intervention should be within the first years of life, if any efficacy were to be expected. In RP patients, SD-OCT imaging provides insight in the remaining structures to be targeted by gene therapy, and is thus useful in determining patient inclusion. Image acquisition is more challenging in severely visually impaired patients, such as those with LCA.

Strengths of this study include the population size and the comprehensive availability of functional and imaging studies, all of which were performed in a very standardized way at a single tertiary referral centre. This allowed for robust statistical analysis – a challenge in rare diseases. Limitations of this study include the retrospective design. The vast genotypic heterogeneity, although representative of the general population, impeded statistical genotype-phenotype analysis. Nonetheless, confirmation of many phenotypic features found in previous large cohorts, and

further substantiation of one genotype-phenotype correlation, indicate that retrospective studies, despite the limitations, provide robust information that is reproducible in different cohorts.

**Funding**

This study was in part funded by the Curing Retinal Blindness Foundation (CJFB), and the Research Foundation Flanders (Belgium) (FWO); Support: FWO Flanders Grant OZP 3G004306 (BPL).

## REFERENCES

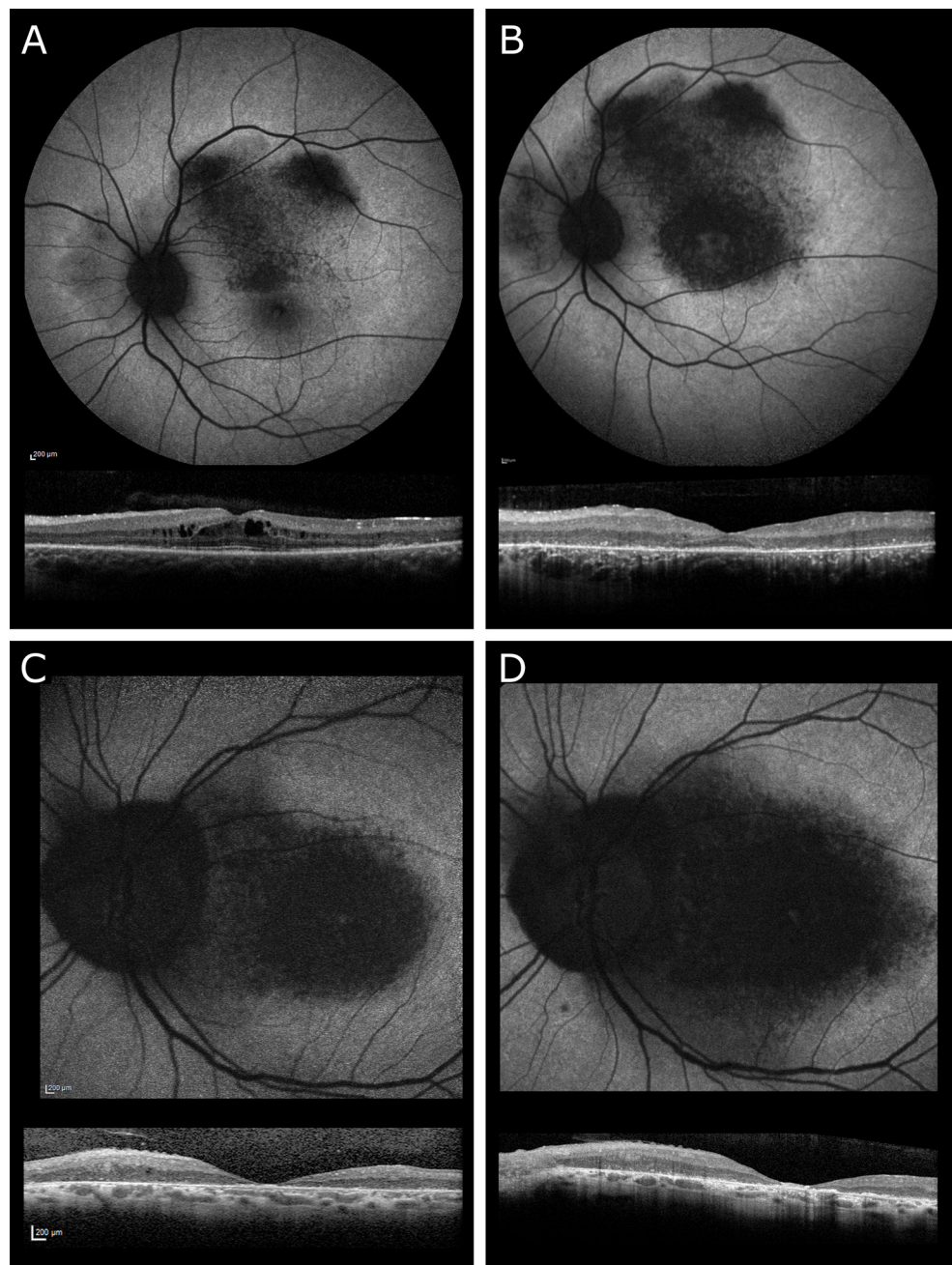
1. Koenekoop RK. An overview of Leber congenital amaurosis: a model to understand human retinal development. *Surv Ophthalmol* 2004;49(4):379-98.
2. Stone EM. Leber congenital amaurosis - a model for efficient genetic testing of heterogeneous disorders: LXIV Edward Jackson Memorial Lecture. *Am J Ophthalmol* 2007;144(6):791-811.
3. Hamel C. Retinitis pigmentosa. *Orphanet J Rare Dis* 2006;1:40.
4. Corton M, Tatu SD, Avila-Fernandez A, et al. High frequency of CRB1 mutations as cause of Early-Onset Retinal Dystrophies in the Spanish population. *Orphanet J Rare Dis* 2013;8:20.
5. Vallespin E, Cantalapiedra D, Riveiro-Alvarez R, et al. Mutation screening of 299 Spanish families with retinal dystrophies by Leber congenital amaurosis genotyping microarray. *Invest Ophthalmol Vis Sci* 2007;48(12):5653-61.
6. Tsang SH, Burke T, Oll M, et al. Whole exome sequencing identifies CRB1 defect in an unusual maculopathy phenotype. *Ophthalmology* 2014;121(9):1773-82.
7. Khan AO, Aldahmesh MA, Abu-Safieh L, Alkuraya FS. Childhood cone-rod dystrophy with macular cystic degeneration from recessive CRB1 mutation. *Ophthalmic Genet* 2014;35(3):130-7.
8. Quinn PM, Pellissier LP, Wijnholds J. The CRB1 Complex: Following the Trail of Crumbs to a Feasible Gene Therapy Strategy. *Front Neurosci* 2017;11:175.
9. Talib M, van Schooneveld MJ, van Genderen MM, et al. Genotypic and Phenotypic Characteristics of CRB1-Associated Retinal Dystrophies: A Long-Term Follow-up Study. *Ophthalmology* 2017;124(6):884-95.
10. Khan KN, Robson A, Mahroo OAR, et al. A clinical and molecular characterisation of CRB1-associated maculopathy. *Eur J Hum Genet* 2018;26(5):687-94.
11. Mathijssen IB, Florijn RJ, van den Born LJ, et al. Long-term follow-up of patients with retinitis pigmentosa type 12 caused by CRB1 mutations: a severe phenotype with considerable interindividual variability. *Retina* 2017;37(1):161-72.
12. Maguire AM, Russell S, Wellman JA, et al. Efficacy, Safety, and Durability of Voretigene Neparvovec-rzyl in RPE65 Mutation-Associated Inherited Retinal Dystrophy: Results of Phase 1 and 3 Trials. *Ophthalmology* 2019;126(9):1273-85.
13. Pellissier LP, Quinn PM, Alves CH, et al. Gene therapy into photoreceptors and Muller glial cells restores retinal structure and function in CRB1 retinitis pigmentosa mouse models. *Hum Mol Genet* 2015;24(11):3104-18.
14. McCulloch DL, Marmor MF, Brigell MG, et al. ISCEV Standard for full-field clinical electroretinography (2015 update). *Doc Ophthalmol* 2015;130(1):1-12.
15. Dagnelie G. Conversion of planimetric visual field data into solid angles and retinal areas. *Clinical Vision Science* 1990;5(1):95-100.
16. Kumaran N, T Moore A, Weleber R, Michaelides M. Leber congenital amaurosis/early-onset severe retinal dystrophy: clinical features, molecular genetics and therapeutic interventions. *Br J Ophthalmol* 2017;101:1147-54.
17. Hettinga YM, van Genderen MM, Wieringa W, et al. Retinal Dystrophy in 6 Young Patients Who Presented with Intermediate Uveitis. *Ophthalmology* 2016;123(9):2043-6.

18. Dutta Majumder P, Menia N, Roy R, et al. Uveitis in Patients with Retinitis Pigmentosa: 30 Years' Consecutive Data. *Ocul Immunol Inflamm* 2018;26(8):1283-8.
19. Yoshida N, Ikeda Y, Notomi S, et al. Clinical Evidence of Sustained Chronic Inflammatory Reaction in Retinitis Pigmentosa. *Ophthalmology* 2013;120(1):100-5.
20. Li, Shen, Xiao, et al. Detection of CRB1 mutations in families with retinal dystrophy through phenotype-oriented mutational screening. *Int J Mol Med* 2014;33(4):913-8.
21. Aredo B, Zhang K, Chen X, et al. Differences in the distribution, phenotype and gene expression of subretinal microglia/macrophages in C57BL/6N (Crb1rd8/rd8) versus C57BL6/J (Crb1wt/wt) mice. *J Neuroinflammation* 2015;12(1):6.
22. McKibbin M, Ali M, Mohamed MD, et al. Genotype-phenotype correlation for leber congenital amaurosis in Northern Pakistan. *Arch Ophthalmol* 2010;128(1):107-13.
23. Hanein S, Perrault I, Gerber S, et al. Leber congenital amaurosis: comprehensive survey of the genetic heterogeneity, refinement of the clinical definition, and genotype-phenotype correlations as a strategy for molecular diagnosis. *Hum Mutat* 2004;23(4):306-17.
24. Jonsson F, Burstedt MS, Sandgren O, et al. Novel mutations in CRB1 and ABCA4 genes cause Leber congenital amaurosis and Stargardt disease in a Swedish family. *Eur J Hum Genet* 2013;21(11):1266-71.
25. Sun W, Zhang Q. A novel variant in IDH3A identified in a case with Leber congenital amaurosis accompanied by macular pseudocoloboma. *Ophthalmic Genet* 2018;39(5):662-3.
26. Testa F, Surace EM, Rossi S, et al. Evaluation of Italian Patients with Leber Congenital Amaurosis due to AIPL1 Mutations Highlights the Potential Applicability of Gene Therapy. *Invest Ophthalmol Vis Sci* 2011;52(8):5618-24.
27. Chacon-Camacho O, Zenteno J. Review and update on the molecular basis of Leber congenital amaurosis. *World J Clin Cases* 2015;3(2):112-24.
28. Lotery AJ, Jacobson SG, Fishman GA, et al. Mutations in the CRB1 gene cause Leber congenital amaurosis. *Arch Ophthalmol* 2001;119(3):415-20.
29. Jacobson SG, Cideciyan AV, Aleman TS, et al. Crumbs homolog 1 (CRB1) mutations result in a thick human retina with abnormal lamination. *Hum Mol Genet* 2003;12(9):1073-8.
30. Pellissier LP, Alves CH, Quinn PM, et al. Targeted ablation of CRB1 and CRB2 in retinal progenitor cells mimics Leber congenital amaurosis. *PLoS Genet* 2013;9(12):e1003976.
31. Mehalow AK, Kameya S, Smith RS, et al. CRB1 is essential for external limiting membrane integrity and photoreceptor morphogenesis in the mammalian retina. *Hum Mol Genet* 2003;12(17):2179-89.
32. Henderson RH, Mackay DS, Li Z, et al. Phenotypic variability in patients with retinal dystrophies due to mutations in CRB1. *Br J Ophthalmol* 2011;95(6):811-7.
33. Coppieters F, Casteels I, Meire F, et al. Genetic screening of LCA in Belgium: predominance of CEP290 and identification of potential modifier alleles in AHI1 of CEP290-related phenotypes. *Hum Mutat* 2010;31(10):E1709-66.
34. den Hollander AI, Heckenlively JR, van den Born LJ, et al. Leber congenital amaurosis and retinitis pigmentosa with Coats-like exudative vasculopathy are associated with mutations in the crumbs homologue 1 (CRB1) gene. *Am J Hum Genet* 2001;69(1):198-203.

35. Shah N, Damani MR, Zhu XS, et al. Isolated maculopathy associated with biallelic CRB1 mutations. *Ophthalmic Genet* 2017;38(2):190-3.
36. Alves CH, Wijnholds J. AAV Gene Augmentation Therapy for CRB1-Associated Retinitis Pigmentosa. *Methods Mol Biol* 2018;1715:135-51.
37. Boon N, Wijnholds J, Pellissier LP. Research Models and Gene Augmentation Therapy for CRB1 Retinal Dystrophies. *Front Neurosci* 2020;14:860.
38. HORAMA. (n.d.). *HORA-001 is in early-stage development for eye diseases caused by defects in the CRB1 gene*. Horama.fr, 2020. Available: <https://www.horama.fr/pipeline/hora-pde6b-2/> [Accessed September 6 2021].



## SUPPLEMENTAL MATERIAL



**Supplementary Figure 1. Progression of degenerative changes in the macula on different imaging modalities in patients with *CRB1*-associated macular dystrophy associated with the p.Ile167\_Gly169del mutation.**  
**A-B.** A male patient between the ages of 24 to 28 years. At the age of 24, dense granular hypo-autofluorescence was seen around the central macula and in the superior part of the posterior pole on the fundus autofluorescence (FAF) image.



Some granular hypo-autofluorescence was seen in nasally from the optic disc. Otherwise, the midperipheral retina showed normal autofluorescence. Spectral-domain optical coherence tomography (SD-OCT) showed parafoveal cystoid macular oedema, and preservation of the central outer nuclear layer. The external limiting membrane and the ellipsoid zone were well-preserved in the fovea, but granular in the peripheral macula. At this time, the full-field electroretinogram showed scotopic and photopic responses within the normal range. The decimal best-corrected visual acuity (BCVA) was 0.6. Four years later, FAF (**B**) showed an increase in the granular hypo-autofluorescence, which had now fully encircled the relatively spared fovea. The SD-OCT showed that the cystoid macula oedema had disappeared, and that the outer nuclear layer and the hyperreflective outer retinal bands were now spared only at the fovea, but severely atrophic elsewhere in the macula. At this stage, the full-field electroretinogram showed a mild rod-cone dystrophy, showing a progression of the isolated macular dystrophy phenotype to a retinitis pigmentosa phenotype. Due to the foveal sparing, the BCVA had not decreased. **C-D**. A male patient between the ages of 28 and 37 years. FAF imaging between the ages of 28 (**C**) and 37 (**D**) years showed an increase of the profound central macula hypo-autofluorescence, with a very small area of relative foveal sparing (BCVA OU: 0.03). The SD-OCT scan showed severe atrophy of the outer retina at baseline, without much change in the peripheral macula through the years (BCVA remained 0.03). A small epiretinal membrane is visible in the nasal macula.

**Supplementary Table 1. Genetic characteristics of patients with CRB1-associated retinopathies**

ID	Allele 1		Allele 2		Diagnosis
	DNA change	AA change	DNA change	AA change	
1	c.2308G>A	p.Gly770Ser	c.2308G>A	p.Gly770Ser	RP + Coats
2	c.3879G>A	p.Trp1293*	c.3074G>A	p.Ser1025Asn	RP
3	c.1892A>G	p.Tyr631Cys	c.4005+1 G>A	Splice	RP
4	c.1256A>G	p.Tyr419Cys	c.2401A>T	p.Lys801*	RP
5	c.929G>A	p.Cys310Tyr	c.1268G>A	p.Cys423Tyr	RP + Coats
6, 7	c.2688T>A	p.Cys896*	c.4135T>C	p.Tyr1379His	RP
8	c.2401A>T	p.Lys801*	c.2401A>T	p.Lys801*	RP + Coats
9	c.929G>A	p.Cys310Tyr	c.1892A>G	p.Tyr631Cys	RP
10	c.2401A>T	p.Lys801*	c.3988del	p.Glu1330Serfs*11	LCA
11	c.2842+5G>A	Splice	c.2843G>A	p.Cys948Tyr	LCA
12	c.2401A>T	p.Lys801*	c.2688T>A	p.Cys896*	LCA
13†	c.3487T>C	p.Cys1163Arg	c.2401A>T	p.Lys801*	RP
14	c.2290C>T	p.Arg764Cys	c.2290C>T	p.Arg764Cys	RP + Coats
15	c.2533_2545del	p.Gly845_Ile1406delinsSerSer	c.2843G>A	p.Cys948Tyr	LCA
16	c.601T>C	p.Cys201Arg	c.601T>C	p.Cys201Arg	RP
17-19†	c.3487T>C	p.Cys1163Arg	c.3487T>C	p.Cys1163Arg	RP, LCA
20	c.2843G>A	p.Cys948Tyr	c.1472A>T	p.Asp491Val	RP
21	c.2533_2539del	p.Gly845Serfs*9	c.2533_2539del	p.Gly845Serfs*9	RP
22†	c.3487T>C	p.Cys1163Arg	c.1349G>A	p.Cys450Tyr	LCA
23	c.2687G>T	p.Cys896Phe	c.2842+5G>A	Splice	RP
24	c.2688T>A	p.Cys896*	c.2688T>A	p.Cys896*	LCA
25	c.1892A>G	p.Tyr631Cys	c.2842+5G>A	Splice	RP
26	c.2842+5G>A	Splice	c.2842+5G>A	Splice	RP
27	c.3307G>A	p.Gly1103Arg	c.3988del	p.Glu1330Serfs*11	RP
28	c.1689C>A	p.Ser563Arg	c.1689C>A	p.Ser563Arg	LCA
29	c.2234C>T	p.Thr745Met	c.2752A>T	p.Ser918Cys	RP
30	c.2498G>A	p.Gly833Asp	c.3879G>A	p.Trp1293*	LCA
31	c.2842+5G>A	Splice	c.4005+1G>A	Splice	LCA
32	c.1084C>T	p.Gln362*	c.1084C>T	p.Gln362*	LCA
33-34	c.498_506del	p.Ile167_Gly169del	c.2401A>T	p.Lys801*	Macular dystrophy
35	c.1084C>T	p.Gln362*	c.2401A>T	p.Lys801*	RP
36	c.498_506del	p.Ile167_Gly169del	c.1084C>T	p.Gln362*	Macular dystrophy
37-38	c.613_619del	p.Ile205Aspfs*13	c.2290C>T	p.Arg764Cys	LCA
39	c.2843G>A	p.Cys848Tyr	c.2842+5G>A	Splice	LCA
40	c.2401A>T	p.Lys801*	c.2688T>A	p.Cys896*	LCA

Patient ID-1 also has a variant of unknown significance (VUS) in *RDH12*: c.635G>A; p.Arg212His. Patient ID-3 also has a VUS in *USH2A*: c.1663C>T; p.Leu555Val.

†These patients are related to each other. They were considered to be from 3 different families, based on the different mutations on the second allele.

**Supplementary Table 2. Patients with asymmetry in visual acuity**

Patient ID	Presumed cause of asymmetry	BCVA better-seeing vs. worse-seeing eye
1	Unilateral Coats-like vasculopathy and a subsequent exudative retinal detachment in the worse-seeing eye	0.05 – LP+ (progression to blindness OU)
3	More atrophy of the foveal ONL in the worse-seeing eye	0.2 – 0.02
5	Unilateral Coats-like vasculopathy in the worse-seeing eye	0.45 – 0.04
9	More CMO and optic disc oedema (initially diagnosed as uveitis) in the worse-seeing eye, with an earlier onset in the worse-seeing eye	0.4 – 0.9 (progression to blindness OU)
11	Unknown, both eyes either blind or severely visually impaired	LP+ – 0.06 (progression to no LP OU)
23	More RPE atrophy (FAF) in the worse-seeing eye, and a very narrow band of RPE sparing in the better-seeing eye. On SD-OCT, both eyes displayed extensive atrophy of the outer retina	0.15 – 0.04
25	An ocular trauma in the worse-seeing eye, which led to an orbital and a cranial fracture	0.8 – LP+
29	More atrophy of the ELM, EZ, and ONL in the worse-seeing eye, a small remnant of foveal sparing remained longer in the better-seeing eye	0.1 – CF (progression to blindness OU)
33	More atrophy of the ELM, EZ, and ONL in the worse-seeing eye (although the better-seeing eye had CMO including in the fovea)	0.05 – 0.6
35	Unknown. More posterior subcapsular cataract in the worse-seeing eye, although not convincingly explanatory for difference in BCVA	0.2 – LP+
36	Unknown (FAF and SD-OCT available only after patient reached blindness in both eyes)	0.25 – 0.08 (progression to blindness OU)
37	More foveal atrophy of ONL in worse-seeing eye	0.03 – 1.00
38	More foveal atrophy of ONL in worse-seeing eye (atrophy of ELM and EZ in both eyes)	0.4-0.63

BCVA, best-corrected visual acuity; CF, counting fingers; CMO, cystoid macular edema; ELM, external limiting membrane; EZ, ellipsoid zone; FAF, fundus autofluorescence; LP, light perception vision; ONL, outer nuclear layer; SD-OCT, spectral-domain optical coherence tomography.

Supplementary Table 3. Treatment histories for cystoid macular oedema in CRB1-associated retinal degenerations

ID	Age during follow-up	Phenotype	Treatment	Treatment duration	Treatment response
3	36-48 years	RP	Oral acetazolamide 250 mg 2dd (at age 36)	15 days	Due to interval censoring (patient visited again after 7 years, age 43), the direct effect on CMO could not be evaluated. CMO had disappeared.
4	11-16 years	RP	None (mild CMO)	-	-
5	54 years	RP + Coats-like exudates OS	- At age 49, a vitrectomy and ILM peeling was performed in OS, due to vitreomacular traction and CMO. - CMO in OD was mild to moderate and was not treated.	-	CMO disappeared after vitrectomy and ILM peeling.
6‡	47 years	RP	None documented (1 <sup>st</sup> visit)	-	-
9	25-49 years	RP (initial differential diagnosis of uveitis)	- Initially (age 25): subconjunctival celestione and topical indometacine and NSAID - A history of mycophenolate mofetil (suspected uveitis), cyclosporine (until the age of 45), and intramuscular ledertrexate (until the age of 46) - Corticosteroids, initially methylprednisolone, then prednisolone 16 mg - Adalimumab injections were initiated at age 45 - Intravenous Infliximab - Intravitreal injections of bevacizumab, several at age 47, restart at age 49 - Oral acetazolamide - Intravitreal injection of triamcinolone at age 48	24 years and ongoing	All medication had an insufficient to no effect on CMO, and the patient still had severe CMO at the final visit. - Oral acetazolamide was discontinued due to side effects - Intravitreal triamcinolone led to elevated intra-ocular pressure, which was treated with intravenous mannitol and topical brinzolamide and latanoprost. A cataract extraction was performed. - Patient developed a renal insufficiency, which was linked to the long-term use of cyclosporine. The renal insufficiency responded well to corticosteroids.
13	0-14 years	RP	None, mild CMO occurred at the age of 12	-	CMO remains mild at the final visit
14	4-22 years	RP + Coats-like exudates OU	Intravitreal triamcinolone OS at age 17	-	Secondary glaucoma OS in response to steroid, with insufficient response to oral acetazolamide, topical bimatoprost and brimonidine/timolol. Glaucoma was then treated with a trabeculectomy with mitomycin C, followed by hypotony. Intra-ocular pressure normalised after intravitreal triamcinolone, followed maintenance with topical brinzolamide/timolol.
16	26 years	RP	Brinzolamide 3dd at age 26	Ongoing	To be evaluated

Supplementary Table 3. Continued

20	4-20 years	RP	None documented (expectative)	-	Persistent CMO during follow-up
23	4-6 years	RP	None (expectative)	-	Persistent CMO during follow-up (age 4-6 years)
33	23-29 years	Macular dystrophy (unilateral CMO, OS)	<ul style="list-style-type: none"> <li>- Initially: intravitreal injection of triamcinolone</li> <li>- Then (ages 25-6) 5 intravitreal injections of bevacizumab</li> <li>- Spironolactone 1dd 50 mg due to a differential diagnosis of atypical CSC*</li> <li>- Age 26: start topical brinzolamide</li> <li>- Age 27: stop brinzolamide, restart intravitreal bevacizumab</li> <li>- Age 27: continue with spironolactone only</li> </ul>	4 years and ongoing	<ul style="list-style-type: none"> <li>- No response to intravitreal triamcinolone</li> <li>- Initial reduction of CMO after the 1<sup>st</sup> bevacizumab injection, but increase of CMO after 2<sup>nd</sup> and 3<sup>rd</sup> injection</li> <li>- Initially no response to spironolactone. In later stages a mild reduction in CMO, so spironolactone was continued. At the final visit, no CMO was found, under usage of only spironolactone.</li> <li>- Mild reduction of CMO after brinzolamide, insufficient response</li> <li>- After restart of bevacizumab, a mild increase in CMO</li> </ul>
34	7-29 years	Macular dystrophy	None (expectative)	-	Spontaneous resolution at age 26 (CMO confirmed on OCT between ages 10-18)
36	23-37 years	Macular dystrophy	Due to the concurrent symptomatic pucker: vitrectomy with ILM peeling, laser and air† at age 37	-	No remaining CMO after vitrectomy
38	4-7 years	RP	None (very mild CMO)	-	-

CMO, cystoid macular oedema; CSC, central serous chorioretinopathy; ILM, inner limiting membrane; NSAID, non-steroidal anti-inflammatory drugs; RP, retinitis pigmentosa.  
 \*No subretinal fluid was found in this patient.

†In one eye. The other eye did not receive treatment.

‡This patient visited the Ghent University Hospital once for a second opinion, and limited information was available on any prior treatment of CMO.



